Investigations into the impact of and mechanisms behind age-associated impaired healing following peripheral nerve injury

Honors Thesis
Presented to the College of Arts and Sciences
Cornell University
in Partial Fulfillment of the Requirements for the
Biological Sciences Honors Program

by

[**William Miklavcic**.]
[**May 24,2020**]

[**Dr. Jonathan Cheetham**]

Abstract:

Peripheral nerve injuries (PNI) present a challenging and debilitating problem to both patients and the healthcare industry . Elderly patients in particular demonstrate a significantly reduced rate of recovery after PNI, prolonging the time they are in pain and immobile. Research into the mechanisms behind these age-associated healing impairments has the potential to unlock new ways to reverse this process and possibly accelerate the rate of recovery for all patients after PNI. Since macrophages and Schwann cells have been shown to be important in peripheral nerve repair, I sought to determine whether age had an effect on their recruitment to the site of a nerve injury. To do this, I first affirmed the impact that age has on both the rate of recovery and extent of full recovery after PNI through the use of hock angle analysis, peak tetanic force (PTF) measurements, and gastrocnemius (gastroc) muscle harvests. I then used novel nerve graft techniques to determine the impact the age of the nerve tissue has on macrophage and Schwann cell recruitment after PNI. While unable to detect age-related differences in rate of recovery after PNI, I found that recovery was similarly incomplete in both old and young animals. My new assay for quantifying macrophage and Schwann cell migration into the injured nerve proved a more convenient, cost-effective method that yielded results challenging previous conceptions by showing macrophage and Schwann cell recruitment was the same between young and old mice.

Introduction:

Research into peripheral nerve injuries (PNI) is a critical field of research in modern medicine. The United States medical care system spends 150 billion dollars every year treating peripheral nerve injuries (PNI) (1). Despite this the probability of full functional

and sensory recovery in treated patients is low. Age of the patient is a key factor in how well the patient recovers after PNI. As a patient ages, the rate at which they heal from PNI decreases significantly (2). As the elderly population is living longer and becoming more dependent on the healthcare system the need for novel treatments of PNI that are more effective than the current standard is growing even greater. It has been well established over the past few decades that humans and mice have similar peripheral nervous systems, both displaying impaired healing ability from PNI with age (3). This allows for mice to serve as a good model for investigating the potential causes of this age-related decline in humans. Experiments investigating the source of age-associated healing impairments have isolated two cell types as key factors in this decline. These two cell types are macrophages and Schwann cells. Schwann cells are cells that encapsulate nerve axons with myelin, a complex of membranes and proteins, that enhances the propagation speed of an electrical impulse along an axon. When the peripheral nerve is injured, Schwann cells are able to switch over from a support phenotype into a repair phenotype. In this new phenotype, Schwann cells play a vital role in peripheral nerve repair through phagocytosing myelin and secreting healing factors. One of these factors is macrophage chemotactic protein 1 (MCP-1) (4). This recruits monocytes from the circulation, causing them to differentiate into macrophages and migrate to the injury site. Macrophages have a myriad of functions that are essential in peripheral nerve repair. Pro-inflammatory macrophages actively clear myelin fragments and other cellular debris occluding the damaged nerve tissue through phagocytosis. Quick and efficient removal of this obstructive debris is critical for maintaining optimal healing conditions from PNI. (5). Anti-inflammatory macrophages in the wound environment release remodeling factors such as Vascular Endothelial Growth Factor A (VEGF-A) and

Transformative Growth Factor β (TGFβ), which both increase Schwann cell remodeling activity (6). Additionally, macrophages secrete factors that further promote Schwann cell activation towards its repair phenotype (6). Increases in activated Schwann cell count and increased Schwann cell activity results in higher levels of axonal regeneration in the wound environment, promoting better long-term recovery (6). Experiments that have investigated the function of these two cell types in both young and old mice have found impaired Schwann cell activation, delayed macrophage recruitment, and higher macrophage infiltration once recruited (7, 8). A better understanding of these impaired processes in aged mice has the potential to unlock new avenues of research and treatments for PNI, especially in the elderly.

To study the age-related impairment of macrophage and Schwann cell infiltration to the injury site, I first set out to replicate and observe the impact that age has on PNI. I used gait analysis methods to observe the impact the age of mice had on changes in the hock angle for fifteen weeks after injury. Monitoring the hock angle after peripheral nerve injury is a good method for non-invasively monitoring the rate and total recovery after PNI in mice (9, 10).

To examine the long-term effects on muscle innervation caused by PNI in young and old mice I performed peak tetanic force (PTF) measurements and gastroc muscle harvests six months after a tibial transection and repair injury in mice. PTF and gastroc mass measurements are strong indicators of both muscle reinnervation and muscle atrophy after PNI (11,12).

In order to investigate the effects of aging on macrophage and Schwann cell recruitment following PNI, I used nerve grafts from young and old mice to observe how the age of

the healing tissue impacts the recruitment of these cells. I quantified macrophage and Schwann cell recruitment into these nerve grafts by counting GFP-tagged macrophages and Schwann cells that infiltrated the nerve graft. Macrophages and Schwann cells were GFP tagged through the use of transgenic mice that express GFP under the S100β promoter. Mice expressing GFP under the S100β promoter have been shown to express GFP-fluorescent macrophages and Schwann cells (13).

My results confirm other reports that young and old mice have similar long-term recovery after PNI. However, in contrast to previous studies, I found that both the rate of recovery after PNI and level of macrophage and Schwann cell migration was not significantly different between young and old mice (7). Despite these results conflicting with other studies, the experiments managed to confirm previously established trends in muscle atrophy displayed in older mice, reinforcing the use of PTF and gastroc mass as valuable metrics for evaluating recovery after PNI. Furthermore, the results of my novel technique for quantifying macrophage and Schwann migration, while incongruous with other published data, highlight a new set of methods that once refined could provide to be a highly efficient, novel tool in the study of immune cell infiltration into wounded nerve tissue.

Methods:

Animals

Two strains of mice were used for this experiment. These strains were C57BL/6 (C57) and S100β-GFP (S100) mice bred on a C57BL/6 background from Jackson Labs. S100β-GFP is expressed on the cell surface of Schwann cells and macrophages in these S100 mice (13). For a mouse to be considered as old it had to be at least 80 weeks old at the

start of the experiment. This criterion is consistently used by PNI studies investigating mice for at this age mice reliably display impaired responses to PNI similar to older human patients. Specifically, after 80 weeks mice begin to display the hallmark delayed macrophage migration, slowed axon growth, and reduced rate of recovery observed in elderly patients suffering from PNI (14, 15).

Hock Angle Evaluation through Gait Analysis

14 C57 mice were used for gait analysis and peak tetanic force (PTF) studies. These 14 mice were five young males, five old males, two young females, and two young males. The old mice were between 122 and 129 weeks old and the young mice were between 14 and 15 weeks old at the time of the initial surgery.

Two weeks prior to the collection of the baseline videos, the fourteen mice were anesthetized using isoflurane and tattooed with black ink on their left stifle, hock, and metatarsal. Preoperative analgesia of 0.05 mL subcutaneous buprenorphine (0.0515 mg/mL) was administered before the tattooing and again 24 hours after the tattooing.

After recovery, the fourteen mice were acclimated to the gait track upon which videos of them walking would be recorded. Acclimatization was achieved by guiding the mice to trot down the gait track five times. This process was repeated on three different days until the mice learned to walk without much resistance down the gait track. At any point if the mouse needed incentive to move down the track, a light blast with an air hose was used to spur the mouse to resume trotting.

Once the mice were tattooed and acclimated, I recorded baseline videos of each mouse running down the track. A high-quality video was defined as one where the mouse maintained a consistent gait speed and stopped infrequently on the track during the run. Five high quality baseline videos were recorded on two separate days for each mouse.

After the baseline videos were collected, the mice were anesthetized and a transection and repair surgery was performed on their left tibial nerves. The mice were given preoperative doses of 0.05 mL buprenorphine (0.0515 mg/mL) and 0.3 mL of warm saline. The surgical site of the mouse was cleaned using betadine and 70% isopropyl alcohol. Mice were induced at 2% isoflurane before being maintained at 1.5% isoflurane.

The sciatic nerve of each mouse was exposed by dissecting through the fascial plane between two muscle bellies of the bicep femoris. The sciatic nerve was followed distally until it bifurcated into the sural, tibial, and common peroneal nerves. After identifying the tibial nerve, the nerve was transected using a #12 scalpel blade before repairing it with two 10-0 ethilon sutures.

After the repair, the nerve was tucked back into its original position and the overlying muscle and skin layers were sutured closed using a 6-0 ethilon suture in a simple continuous pattern.

All fourteen mice were monitored after the surgery. Post-operative buprenorphine was administered after 24 hours and each mouse was weighed daily for 48 hours. The following criteria was used to monitor the health of the mice after surgery. If any mouse lost more than 10% body weight, 0.3 mL of warm saline was administered. If the mouse

lost more than 20% of its body weight, it was euthanized. However, no mice required any saline treatments during the recovery window.

One week after the surgery, videos were collected of each mouse running down the gait track. Videos were recorded until five high quality videos were collected each week and this was repeated for 15 weeks. Three of the five recorded videos for each week were selected based off of the consistency in mouse speed, appropriate gait, and level of resolution in each video. Then, the hock angle was determined through further analysis in Simi Motion Analysis software. For each of these videos, the hock angle of the left leg during midstance was measured at three different time points within the video (Figure 1) . The average hock angle from three videos was determined for every week and normalized to the baseline hock angle. This data was then plotted in GraphPad Prism 8.0 to evaluate the rate of recovery in young and old mice.

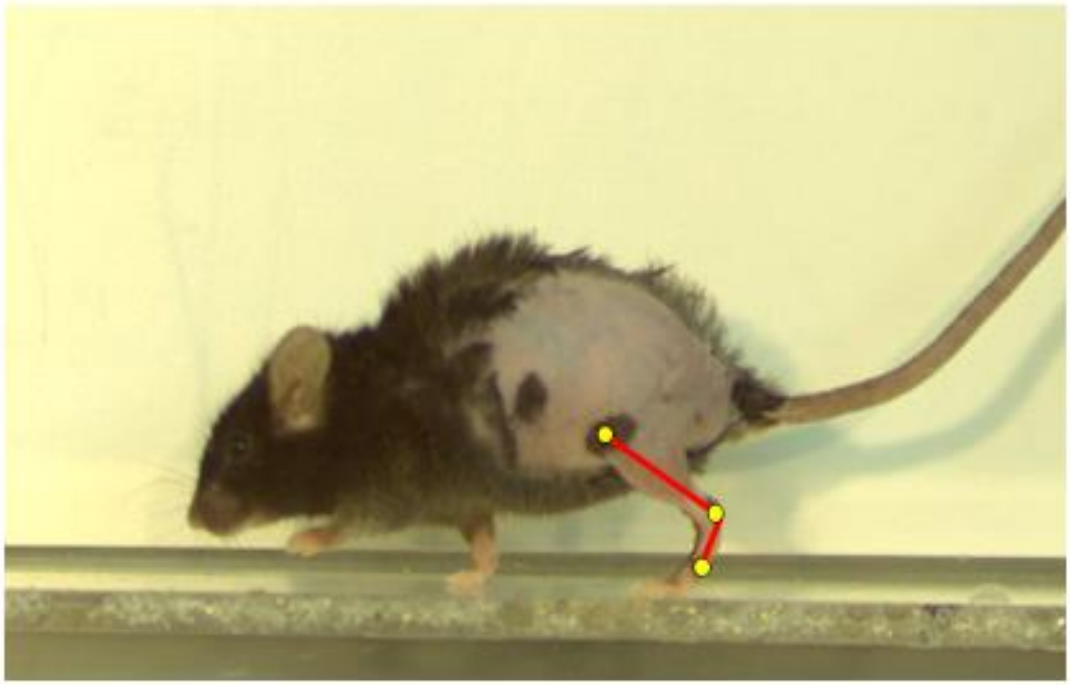

Fig 1.

Example of the angle measured to determine the hock angle. These two lines are connecting the hip (top), stifle (middle), and metatarsal (bottom). Mouse is currently in midstance.

Peak Tetanic Force Measurements and Gastrocnemius Harvests

After collecting the gait data, I determined PTF and gastroc harvests as an additional metric to quantify the total recovery of each mouse. By this time, only nine of the mice remained due to deaths that occurred naturally or accidentally during the collection of the videos. To collect the PTF measurements, each mouse was anesthetized using isoflurane and wrapped in a tin foil blanket to preserve body heat. I then surgically isolated the sciatic nerve using the same method as the first surgery. The tibial, common peroneal, and sural branches of the sciatic nerve were identified, and the common peroneal and sural nerves were transected. I then isolated the gastroc muscle from the

surrounding tissue and excised the calcaneus from the hock. A circumferential silk 3-0 suture was placed around the common calcaneal tendon and attached to the force lever (Cambridge Technology Inc. Model 6650LR).

I repeated the entire procedure on the right leg of the mouse as an internal control to mitigate the differences between young and old mice in muscle composition.

After both surgeries, the mouse was moved from the surgical site to the force lever apparatus (Cambridge Technology Inc. Model 6650LR). The mouse was mounted to the platform by pinning the left tibial crest between two screws and by tying the silk suture of the left gastroc muscle to the force lever. Electrodes were placed approximately 5 mm apart on the isolated sciatic nerve. I stimulated the sciatic nerve with 100 Hz at 1.5 mA to titrate the optimal tension on the gastroc muscle from the force lever. After optimizing this distance, I took three PTF measurements at 1.5 mA using 100Hz stimulation frequency in a biphasic pulse. A five-minute recovery period was observed after each measurement in order to allow the muscle to recover. After collecting three PTFs on the left side, the same measurements were recorded on the right side. Once PTF measurements were recorded for the left and right sides, the mouse was euthanized and the left and right gastroc muscles were harvested and their weights recorded. Due to the duration and complexity of these experiments, only two young mice and two old mice survived long enough during the surgeries to yield complete data sets for PTF. In the event that a mouse died before complete collection of the PTF values, the gastroc muscles were still harvested and weighed.

All data collected from the PTF and from the gastroc muscle harvests was analyzed in GraphPad 8.0.

Macrophage and Schwann Cell Infiltration

To determine the degree of macrophage and Schwann cell migration within the injury site I used transgenic mice expressing GFP under the S100β promoter.

Twelve S100 mice received 1 cm sciatic nerve grafts from donor C57 mice (Figure 2). Six of the donor nerves were from young mice (between 11 and 14 weeks) and six of the donor nerves were from old mice (90+ weeks). The sciatic nerve was exposed as described above. The donor mouse was euthanized before exposing and harvesting both its left and right sciatic nerves. These grafts were kept moist by keeping them in the donor mouse's muscle cavity until the host mouse was ready to receive the graft. The host mouse's sciatic nerve was transected once, and the 1 cm donor segment was grafted between the two severed ends. Both the host's proximal and distal sciatic stumps were sutured into the donor graft. One mouse did not survive the surgery, bringing the experimental design to five young nerve grafts compared to six old nerve grafts.

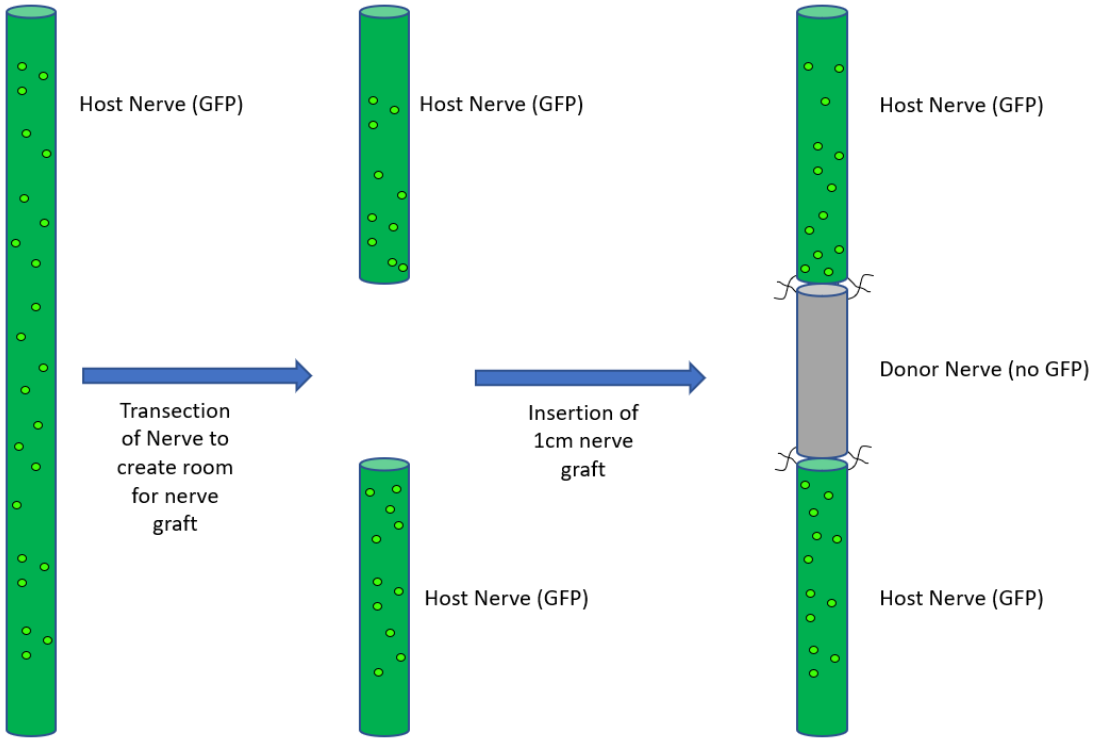

Fig 2.

Diagram of nerve graft implantation in S100 mouse. From left to right, intact recipient nerve, transected recipient nerve, and recipient nerve repaired with 1 cm nerve graft from C57 donor mouse.

After six days, I harvested the entire nerve graft including several millimeters proximal and distal of the nerve graft. The isolated nerve grafts were fixed overnight in 4% PFA before being sectioned longitudinally and mounted in an aqueous mounting solution with a cover slip. Within 72 hours of mounting, all 11 nerve grafts were imaged underneath a wide field fluorescence microscope. An image of the proximal and distal nerve junctions with the nerve graft was captured at 40X magnification, and a more detailed strip across these junctions was captured at 100X.

I created a region of interest in the 100x nerve graft image to count macrophage and Schwann cell recruitment. In Image J a line was traced along the border of the host nerve with the donor nerve, and this line was displaced by 200 pixels into the nerve graft (204.4 μm). This number was selected as it was the largest consistent area I could capture within the nerve graft that was not clipped by the border of the image. All distinct fluorescent objects were counted within this region of interest. Macrophage and Schwann cell count was then divided by the area of the region of interest to determine a relative density of macrophages and Schwann cells within the nerve graft. All data was processed and analyzed for statistical significance in Graphpad Prism 8.0.

Statistics

All statistics were performed in GraphPad Prism 8.0. All data sets were confirmed to be normally distributed through Shapiro-Wilks testing unless otherwise mentioned. All unpaired t-tests were conducted after establishing parametric distribution of data and all unpaired t-tests assumed the same standard deviation of data across each group, without using Welch's correction.

Hock angle analysis data was averaged for each week before being normalized to the baseline hock angle. This was plotted over fifteen weeks to show the change in hock angle throughout the recovery period from PNI. Standard error of mean bars were included below each point to help demonstrate variability in the data. A two-way ANOVA test comparing young and old mice over the 15 weeks of the experiment yielded an insignificant p-value of 0.169.

PTF and gastroc harvest data was analyzed for statistical significance. The ratio of the left leg vs right PTF divided by gastroc mass data was plotted for both young and old mice. These data were too small to be confirmed normally distributed through Shapiro-Wilks testing, but it was analyzed using an unpaired t-test which yielded a p-value of 0.5326. The ratio of left gastroc mass to right gastroc mass between young and old mice was analyzed using an unpaired t-test which revealed a p-value of 0.583. An unpaired t-test of the ratios of left vs right leg PTF between young and old mice yielded a p-value of 0.6903, however this data set was too small to test for normal distribution using Shapiro-Wilks testing. An unpaired t-test comparing the ratio of young and old right gastroc mass to body weight yielded a p-value of 0.0254.

Macrophage and Schwann cell count within the region of interest of the sciatic nerve grafts was calculated as a density by dividing by the area of the region of interest. At this point only data for nine complete nerve grafts was available due to complications mounting and processing two of the samples. Two densities were measured for each nerve graft corresponding to the proximal and distal boundary regions. An unpaired t-test compared the cell densities of young and old nerve graft, averaging the cell counts of the proximal and distal nerves for each animal. This resulted in a p value of 0.4122. Further investigation using unpaired t-tests comparing the ratio of proximal to distal cell counts in young versus old nerve grafts yielded a p-value of 0.0828. A paired t-test comparing the cell densities between proximal and distal regions of interest in the nerve grafts independent of age, generated a p value of 0.7824.

The experimental design allowed me to compare macrophage and Schwann cell recruitment between male and female recipient mice. This was done by reorganizing the

already collected data into different groups: five male host mice which had received three young nerve grafts and two old nerve grafts were clumped together, while four host female mice receiving two young nerve grafts and two old nerve grafts were grouped together. An unpaired t-tests comparing the ratio of proximal to distal cell densities in male and female hosts generated a p value 0.1507.

Results:

GFP-tagged macrophages and Schwann cells infiltrated both young and old nerve graft tissue with similar density in both the proximal and distal stumps.

I studied the impact that the age of nerve graft tissue had on infiltration of macrophages and Schwann cells by grafting unstained C57 sciatic nerve grafts into S100 mice. Eleven young S100 mice were given nerve grafts from five young and six old donor C57 mice. After six days these nerve grafts were harvested and widefield fluorescence microscopy was used to capture longitudinal images of the proximal and distal borders of the nerve graft. Using Image J, I counted all distinct fluorescent bodies in the nerve graft within a region of interest. This region of interest was delineated as the area of graft tissue within 204.4 μm of the host-graft nerve boundary (Figure 3). The macrophage and Schwann cell count was then calculated as cell density by dividing by the area of the region of interest. No differences in macrophage or Schwann cell infiltration were observed between young and old nerve tissue grafts (Figure 4). Furthermore, no statistically significant differences were observed in the infiltration of macrophages and Schwann cells between proximal or distal stumps, regardless of the age of the nerve graft (Figure 4).

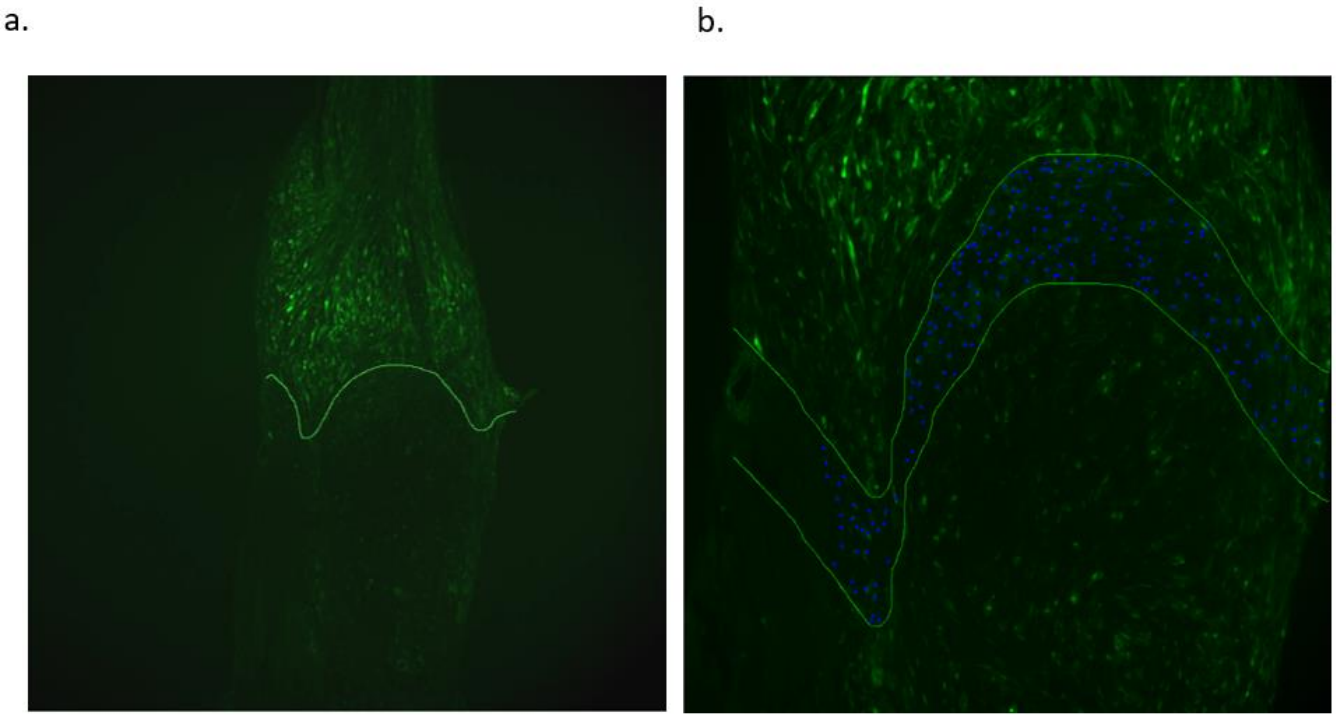

Fig .3

Image of fluorescence microscopy images of nerve grafts. ***a****. Shows 40x magnification of the proximal boundary between the S100 nerve (top of line) and C57 nerve (bottom of line).* ***b****. Shows the 100x magnification image where the region of interest is illustrated and the cells are being counted within that region.*

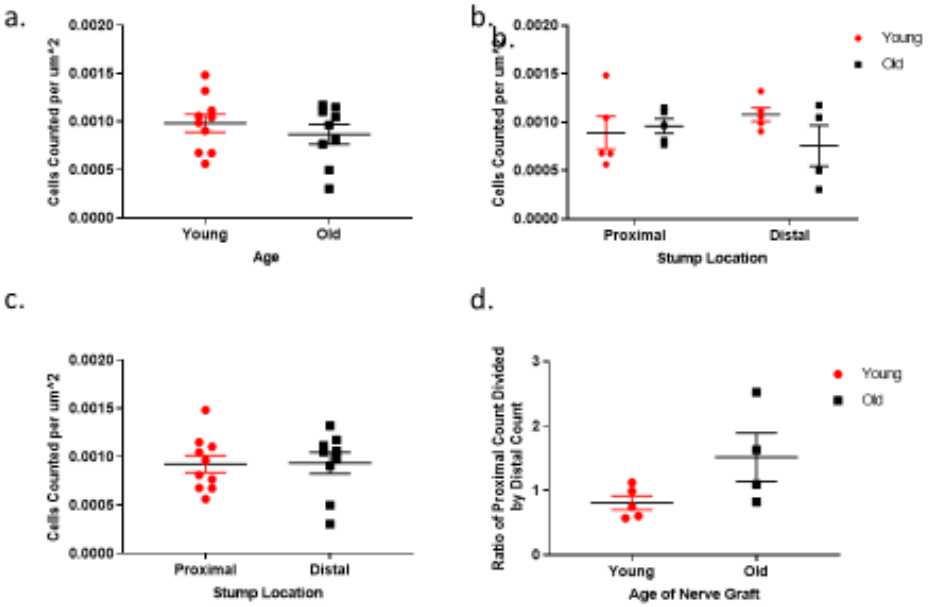

Fig .4

Cell densities determined from quantification of fluorescent macrophages and Schwann cells that migrated into the proximal and distal regions of the nerve graft. ***a.*** *Average macrophage and Schwann cell density in the nerve graft grouped based on age of the nerve graft.* ***b.*** *Cell density of macrophage and Schwann cell infiltration into nerve graft based on both age of graft and location within nerve graft.* ***c.*** *Cell density of macrophages and Schwann cell infiltration into nerve graft grouped by location within nerve graft.* ***d.*** *Comparison of ratio of macrophage and Schwann cell infiltration into proximal stump compared to distal stump between young and old nerve graft tissue.*

Interestingly some statistically insignificant differences were observed in macrophage and Schwann cell infiltration dependent on the sex of the recipient mouse. While not statistically significant, these observations were calculated to have a p value of 0.1507, which indicates a potential area for future investigation (Figure 5).

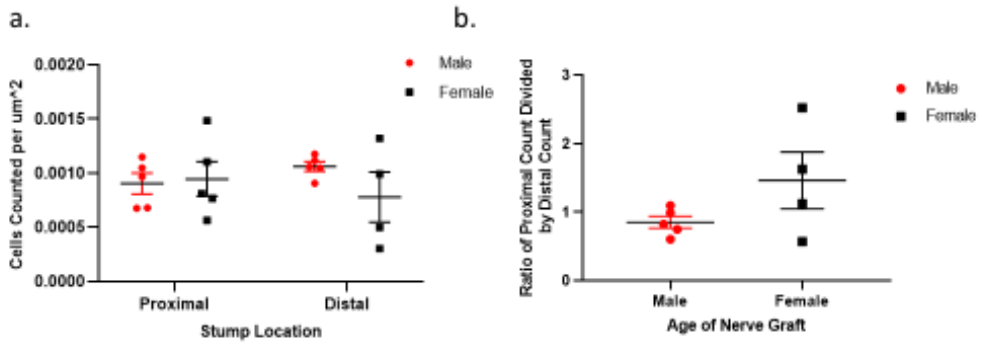

Fig .5

Cell densities determined from quantification of fluorescent macrophages and Schwann cells that migrated into the nerve graft. ***a.*** *Cell density of macrophage and Schwann cell infiltration into nerve graft based on both sex of recipient mouse and location within nerve graft.* ***b.*** *Comparison of ratio of macrophage and Schwann cell infiltration into proximal stump compared to distal stump between male and female mouse recipients.*

Hock angle measurements after tibial nerve injury and repair demonstrated no differences between young and old mice in both rate of recovery and extent of recovery.

To evaluate the ability of young and old mice to recover from a peripheral nerve injury I plotted the changes in the mouse's hock angle at midstance for 15 weeks after a tibial injury. Hock angles were measured using SIMI gait software as described above. The

average hock angle for each week was normalized to an average baseline hock angle recorded prior to tibial nerve injury and repair (Figure 6). This data represents average values for young and old mice plus and minus standard error of mean measurements plotted over 15 weeks. The data reflected the expected decrease in hock angle after tibial nerve injury and repair. Over 15 weeks, this angle gradually increased towards the original baseline value, plateauing at approximately 65% recovery of baseline hock angle. No apparent differences were observed between young and old mice in both the rate of recovery and extent of total recovery after over the 15 weeks of the experiment.

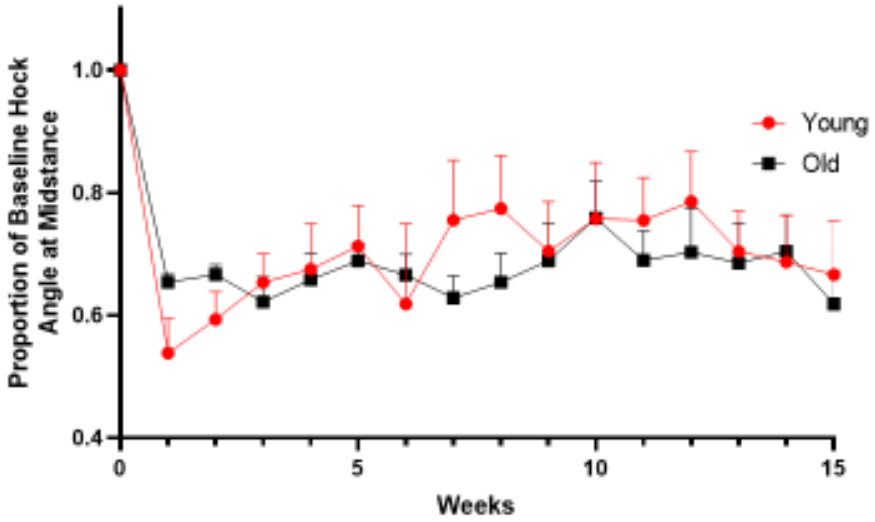

Fig .6

Mouse hock angle measured weekly after tibial injury and represented as a proportion of the average baseline hock angle prior to injury. Measured for 15 weeks post-injury to assess the rate of recovery of the two age groups from PNI. Bars represent standard error of mean. Work for this figure done in conjunction with Kareena Sagar.

Peak tetanic force measurements and gastrocnemius masses collected from eleven mice six months after a tibial transection and repair illustrated no differences between young and old mice in extent of total muscle recovery.

To study the extent of final muscle recovery after peripheral nerve injury, eleven mice were evaluated six months after receiving a tibial transection and repair injury on their left leg. These mice had been previously used in a gait analysis experiment. I measured the peak tetanic force of both the left and right gastroc muscles before harvesting and weighing the gastroc muscles. The peak tetanic force data was normalized to the gastroc mass to determine the force per gram of muscle. Comparing the peak tetanic force per gram of gastroc muscle between both the injured left leg and the control right leg showed no statistically significant differences between young and old mice (Figure 7). This demonstrated that the level of reinnervation of the gastroc muscle after injury was similar in both young and old mice. The ratio of left gastroc mass to right gastroc mass similarly showed no statistically significant differences between young and old mice, indicating that similar levels of muscle atrophy occurred in both age groups after tibial injury (Figure 7). In old mice the ratio of the right gastroc muscle mass to animal body weight was significantly less than the ratio in young mice (Figure 7). This difference in the relative size of the gastroc muscle to overall body weight is expected due to increases in muscle atrophy and body fat in aged mice. Comparison of the peak tetanic force per gram of gastroc muscle on the right leg showed no differences between young and old mice, indicating that uninjured muscles in young and old mice have similar levels of strength relative to gram of muscle (Figure 7).

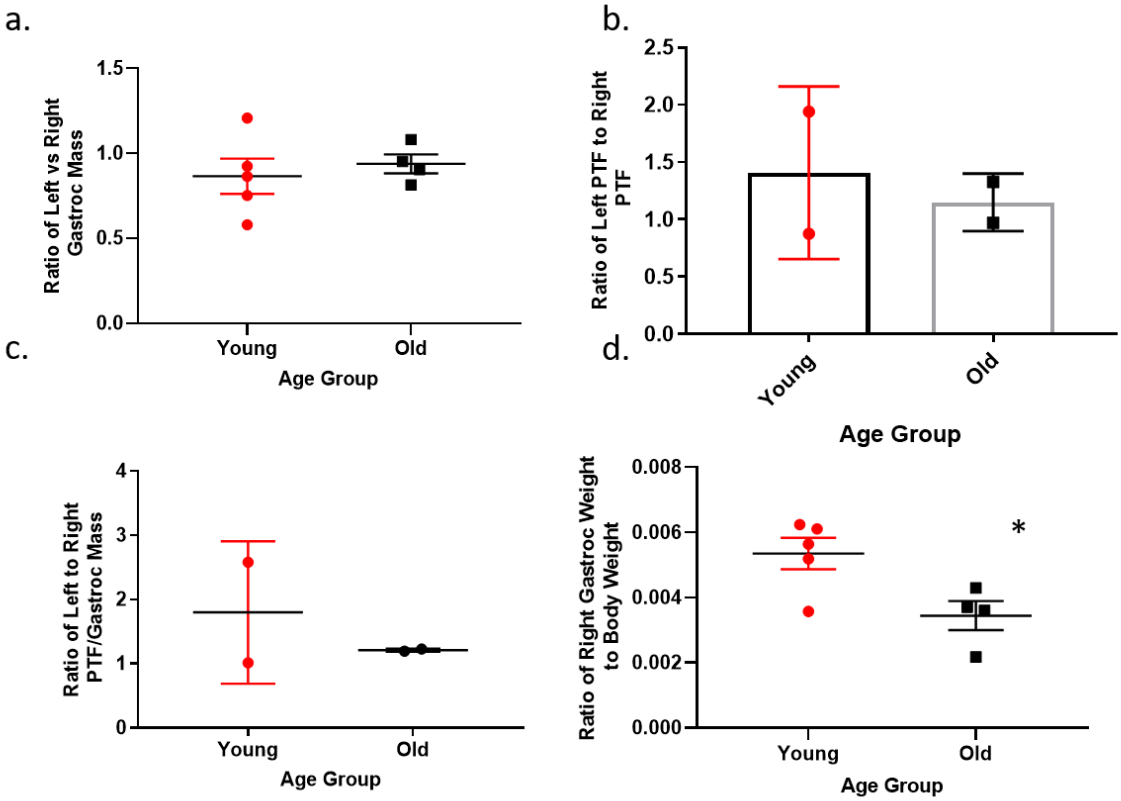

Fig .7

Analysis of peak tetanic force ratios, gastroc mass ratios, and body weight to ascertain extent of total recovery after tibial injury. ***a.*** *Ratio of left leg vs right leg gastroc mass to determine total reinnervation of muscle after injury.* ***b****. Comparison of the ratio of the left vs right peak tetanic force recorded for young and old mice.* ***c.*** *Peak tetanic force divided by gastroc mass as a ratio between left and right legs.* ***d.*** *Right leg gastroc mass as a proportion of body weight. Demonstrates natural ratio of uninjured muscle to total body weight of animal. Work for this figure done in conjunction with Kareena Sagar.*

Discussion:

In this study I investigated the impact that the age of a mouse has on both the mechanisms driving peripheral nerve repair as well as the rate and extent recovery of the mouse following PNI. My experiments demonstrated that young and old mice do not have statistically significant different rates of recovery, total recovery, or macrophage and Schwann cell infiltration into the injured nerve after PNI. My finding that young and old mice have similar extents of total recovery after PNI is a finding supported by

other investigators using different methods. Several papers have been published that demonstrate differences in the rate of recovery after PNI are present between young and old mice, which conflicts with my other set of results (2, 7, 8). Additionally, other investigators have determined that macrophages are recruited at different levels based on the age of the host after a peripheral nerve injury (7). These discrepancies between the results in this paper and with other investigators indicates further research needs to be conducted to determine how the variations in the type of models I used contributed to these observed differences.

The use of hock angle as a metric for analyzing the rate of recovery from PNI is well established (9, 10). Furthermore, differential rates of recovery after PNI based on the age of the animal has also been shown through the use of sensory pinprick scores, axon count, and peak tetanic force measurements (2, 7, 8). Therefore, I expected my hock angle analysis metrics to have shown different rates of recovery between the age groups. There are several potential reasons for why I had difficulty in replicating these results. First, I had some difficulty with the mice throughout the experiment in trying to get them to successfully run the GAIT analysis track. Prior to the PNI, the mice would reluctantly run down the track at a relatively consistent speed, however in the weeks after the surgery the mice were resistant to running on the track. This manifested through mice adopting a more stop-and-go manner of running as well as sporadically alternating between normal and crouched-like walking styles, which significantly increased difficulty to record and analyze videos. For example, if the mouse was in a more crouched stance for a video, then the hock angle would inherently be decreased, thus potentially resulting in an artificially low hock angle. While I limited the videos I

analyzed to ones where the mouse ran consistently and in a normal stance, such selection potentially impacts the results. Another factor that could explain how I observed similar rates of recovery in both age groups is that my sample sizes were not large enough to detect a small difference in the rate of recovery. Replicating this study with more mice may allow better statistical power to identify significant results.

One important finding of my study is that I observed a plateau in recovery after tibial nerve injury, with both young and old mice only healing to ~65% baseline hock angle at 15 weeks after injury. This indicates that the extent of functional recovery after tibial injury and repair is limited. Similar findings have been shown in other papers and is believed to be the result of re-growing tibial axons asynchronously reinnervating wrong muscle fibers or hyper-innervating the correct muscle fibers (11,17). My findings of incomplete functional recovery after PNI is similar to those of found by other investigators, confirming the validity of my approach through the use of hock angle analysis to measure the extent of full functional recovery in mice (17,18).

My use of PTF measurements and gastroc weights confirmed that young and old mice have similar levels of muscle recovery after PNI. However, for this experiment the small sample size of two young compared to two old is a hindrance in determining any significant differences. The original plan of using seven old mice and seven young mice in this experiment was disrupted by the death of two young mice and three old mice during the six-month recovery window. These mice died due to medical complications over the length of the experiment. The remaining mice were lost due to complications in the data harvest as a result of the complex nature of the procedure. While the study may

be viewed as preliminary given the small group numbers, the results do demonstrate the validity of this approach.

Despite difficulties in sample size, the data collected from the PTF and gastroc harvests was important. I was able to show that both young and old mice had similar levels of muscle recovery after injury and that the force per gram of muscle of the left legs was not statistically different than that of the uninjured right legs. These similar levels of muscle reinnervation between injured and uninjured legs do not indicate complete functional recovery in the mice, but simply that each muscle is reinnervated. It has been demonstrated by other researchers that maximal contractive forces are restored after PNI-induced atrophy but that they do not indicate functional recovery (11, 17, 19). Research has found that hyperinnervation of the gastroc muscle after PNI allowed the muscle to contract with similar force to the uninjured leg, but that this contraction was asynchronous with nerve stimulation. Muscle contraction asynchronous with nerve stimulation results in the loss of fine motor control, which explains how the hock angle analysis data showed a plateau in functional recovery while my PTF and gastroc data showed almost complete recovery of the contractive force of the muscle. Confirmation of these findings using my PTF and gastroc mass methods reinforces the validity of my results. I also found that young mice have proportionately larger gastroc muscles than older mice, reflecting increased muscle atrophy in older mice, findings that replicate results elsewhere (20-22). Verification of these trends using gastroc harvest techniques further validates the reliability of my methods in being able to accurately measure muscle atrophy after injury.

My novel technique using longitudinally sectioned peripheral nerve grafts to quantify macrophage and Schwann recruitment after PNI suggests that the age of the donor tissue has no impact on the number of Schwann cells and macrophages recruited to the wound site. This finding is contradictory to investigations by Painter et al. (2014) that showed macrophage recruitment was significantly delayed in aged tissues for the first seven days after PNI (7). In their studies, Painter et al. demonstrated this by staining all macrophages using a CD68+ marker and calculating the total fluorescence relative to the cross-sectional area of the damaged nerve. My method was different in that I used longitudinally sectioned samples from the center of the nerve and quantified GFP-tagged macrophages and Schwann cells by counting all distinct fluorescent bodies within a specific area. While I was able to detect both macrophages and Schwann cells in S100 mice, it is unlikely that many Schwann cells were counted since it is atypical behavior for Schwann cells to migrate into the site of peripheral nerve injury (4, 13, 23, 25). Typically, the Schwann cells already at the injury site recruit macrophages to the wound to aid in repair. Therefore, by counting only cells within the region of interest of the C57 nerve graft, I likely quantified mostly macrophages. This allows for a strong comparison between my results and the results of Painter et al (2014).

My different method for macrophage detection is a likely source for my conflicting results. Painter's method of staining the macrophages after nerve graft harvest introduces the chance of not detecting all the macrophages in the tissue. While CD68+ is a strong pan-macrophage marker, it is possible during the staining process that CD68+ markers were denatured or did not permeate properly, limiting the number of macrophages that could be detected. Using GFP-S100B intrinsically fused to all

macrophages reduces these risks. However, GFP is liable to denature over time and with exposure to light so this method is also not perfect. But by imaging all samples within 72 hours of harvesting I aimed to mitigate this loss of GFP over time. While unable to directly make comparisons to studies that only quantify Schwann cell migration, the convenience and simplicity of this newly developed protocol indicates that it has much potential in future studies. Further research verifying and fine-tuning this method, specifically with a focus on distinguishing between macrophages and Schwann cells within the nerve graft, could allow for this method to be molded into a powerful new tool in the study of PNI in mice.

An interesting byproduct of my studies concerning macrophage and Schwann cell migration into nerve grafts after PNI are potential trends indicating differential macrophage and Schwann cell infiltration between proximal and distal ROI dependent on the age of the nerve graft and the sex of the recipient mouse. I calculated a p-value of 0.0828 when comparing the ratio of infiltrating macrophages and Schwann cells across proximal and distal graft ROIs between young and old nerve graft tissue. Additionally, I observed a p-value of 0.1507 when comparing the ratio of macrophages and Schwann cell densities in proximal versus distal nerve graft ROIs between male and female recipient mice. While not statistically significant, these p-values indicate potential trends in macrophage and Schwann cell recruitment that further experiments with an increased sample size could potentially detect.

Moving forward, I will tentatively approach any future GAIT analysis studies including aged mice due to the difficulty I had in getting them to run properly. Future GAIT analysis experiments including old mice will emphasize developing better ways to

motivate the mouse to run down the track. This might include a longer training window before starting the experiment, using a reward at the end of the track for positive feedback, or even using a stronger positive punishment to spur the mouse down the track.

Other assay systems are also useful in studying recovery of function that do not encounter the same limitations I encountered with GAIT analysis. I will continue to refine my PTF and gastroc harvest protocols for future experiments in order to reduce the difficulty of data collection so that when the experiments are replicated less mice will be lost. Finally, I will continue to develop and experiment with my macrophage and Schwann cell recruitment assay as it was significantly quicker and easier than other previously attempted methods to determine macrophage and Schwann cell recruitment. A future experiment would be to quantify the area of fluorescence relative to the area of the nerve instead of simply counting each distinct fluorescent body. In addition, harvesting nerve grafts at various times after recovery would allow me to identify changes in macrophage and Schwann cell recruitment occur over time in both young and old mice. These modifications to the protocol may help resolve differences between my observations and those of other authors

In this paper I was able to use PTF and gastroc harvests to corroborate findings that young and old mice display similar levels of muscle reinnervation after tibial nerve injury. My use of hock angle analysis showed that both young and old mice do not regain full functional recovery after a tibial nerve injury while also indicating that their rates of recovery after PNI were similar. Finally, the novel technique I used for quantifying macrophage and Schwann cell migration into peripheral nerves yielded data that

challenged previously accepted knowledge by showing that macrophage and Schwann cell recruitment into injured nerves was independent of the age of the nerve tissue. While still preliminary, these findings illuminate new areas in which to investigate the mechanisms behind age-associated impaired recovery from PNI. With enough time, research, and experimentation, breakthroughs can be made from research like this that can revolutionize treatments for PNI for all ages.

Acknowledgements:

I would like to thank my P.I., Dr. Jonathan Cheetham for guidance and support throughout the thesis. I would also like to thank the lab manager, Michael Sledziona, for his constant assistance and help in troubleshooting any issues that cropped up. I would also like to thank Dr. Fiona Ingilis, a postdoctoral associate in the lab who was instrumental in helping write this thesis. Finally, I would like to thank Kareena Sagar, an undergraduate student who worked on some of these experiments with me. This work was by an RO1 grant from the National Institute for Deafness and Communication Disorders.

References:

1. Grinsell, D., & Keating, C. P. (2014). Peripheral nerve reconstruction after injury: a review of clinical and experimental therapies. *BioMed Research International*, *2014*, 698256. https://doi.org/10.1155/2014/698256
2. Kovačič, U., Sketelj, J., & Bajrović, F. F. (2009). Chapter 26 Age-Related Differences in the Reinnervation after Peripheral Nerve Injury. *International Review of Neurobiology*, *87*, 465–482. https://doi.org/10.1016/S0074-7742(09)87026-8
3. Angius, D., Wang, H., Spinner, R. J., Gutierrez-Cotto, Y., Yaszemski, M. J., & Windebank, A. J. (2012). A systematic review of animal models used to study nerve regeneration in tissue-engineered scaffolds. *Biomaterials*, *33*(32), 8034–8039. https://doi.org/10.1016/j.biomaterials.2012.07.056
4. Tofaris, G. K., Patterson, P. H., Jessen, K. R., & Mirsky, R. (2002). Denervated Schwann Cells Attract Macrophages by Secretion of Leukemia Inhibitory Factor (LIF) and Monocyte Chemoattractant Protein-1 in a Process Regulated by Interleukin-6 and LIF. *The Journal of Neuroscience*, *22*(15), 6696–6703. https://doi.org/10.1523/JNEUROSCI.22-15-06696.2002
5. Novak, M. L., & Koh, T. J. (2013). Macrophage phenotypes during tissue repair. *Journal of Leukocyte Biology*, *93*(6), 875–881. https://doi.org/10.1189/jlb.1012512
6. Chang, F., Wang, Y., Liu, P., Peng, J., Han, G.-H., Ding, X., … Huang, K. (2018). Role of macrophages in peripheral nerve injury and repair. *Neural Regeneration Research*. https://doi.org/10.4103/1673-5374.253510
7. Painter, M. W., Brosius Lutz, A., Cheng, Y. C., Latremoliere, A., Duong, K., Miller, C. M., Woolf, C. J. (2014). Diminished Schwann cell repair responses underlie age-associated impaired axonal regeneration. *Neuron*, *83*(2), 331–343. https://doi.org/10.1016/j.neuron.2014.06.016
8. Scheib, J. L., & Höke, A. (2016). An attenuated immune response by Schwann cells and macrophages inhibits nerve regeneration in aged rats. *Neurobiology of Aging*, *45*, 1–9. https://doi.org/10.1016/j.neurobiolaging.2016.05.004
9. Lin, F. M., Pan, Y. C., Hom, C., Sabbahi, M., & Shenaq, S. (1996). Ankle stance angle: A functional index for the evaluation of sciatic nerve recovery after complete transection. *Journal of Reconstructive Microsurgery*, *12*(3), 173–177. https://doi.org/10.1055/s-2007-1006472
10. Rui, J., Runge, M. B., Spinner, R. J., Yaszemski, M. J., Windebank, A. J., & Wang, H. (2014). Gait cycle analysis parameters sensitive for functional evaluation of peripheral nerve recovery in rat hind limbs. *Annals of Plastic Surgery*, *73*(4), 405–411. https://doi.org/10.1097/SAP.0000000000000008
11. Gordon, T., Tyreman, N., & Raji, M. A. (2011). The basis for diminished functional recovery after delayed peripheral nerve repair. *Journal of Neuroscience*, *31*(14), 5325–5334. https://doi.org/10.1523/JNEUROSCI.6156-10.2011
12. Li, Q. T., Zhang, P. X., Yin, X. F., Han, N., Kou, Y. H., Deng, J. X., & Jiang, B. G. (2013). Functional Recovery of Denervated Skeletal Muscle with Sensory or

Mixed Nerve Protection: A Pilot Study. *PLoS ONE*, *8*(11), e79746. https://doi.org/10.1371/journal.pone.0079746
13. Tomlinson, J. E., Golshadi, M., Donahue, C. J., Dong, L., & Cheetham, J. (2020). Evaluation of two methods to isolate Schwann cells from murine sciatic nerve. *Journal of Neuroscience Methods*, *331*, 108483. https://doi.org/10.1016/j.jneumeth.2019.108483
14. Verdú, E., Ceballos, D., Vilches, J. J., & Navarro, X. (2000). Influence of aging on peripheral nerve function and regeneration. Journal of the Peripheral Nervous System, 5(4), 191–208. https://doi.org/10.1111/j.1529-8027.2000.00026.x
15. Büttner, R., Schulz, A., Reuter, M., Akula, A. K., Mindos, T., Carlstedt, A., … Morrison, H. (2018). Inflammaging impairs peripheral nerve maintenance and regeneration. *Aging Cell*, *17*(6). https://doi.org/10.1111/acel.12833
16. Fu, S. Y., & Gordon, T. (1995). Contributing factors to poor functional recovery after delayed nerve repair: Prolonged denervation. *Journal of Neuroscience*, *15*(5 II), 3886–3895. https://doi.org/10.1523/jneurosci.15-05-03886.1995
17. Gillingwater, T. H., Thomson, D., & Ribchester, R. R. (2004). Myo-GDNF increases non-functional polyinnervation of reinnervated mouse muscle. *NeuroReport*, *15*(1), 21–25. https://doi.org/10.1097/00001756-200401190-00006
18. Fey, A., Schachner, M., & Irintchev, A. (2010). A Novel Motion Analysis Approach Reveals Late Recovery in C57BL/6 Mice and Deficits in NCAM-Deficient Mice after Sciatic Nerve Crush. *Journal of Neurotrauma*, *27*(5), 815–828. https://doi.org/10.1089/neu.2009.1217
19. Magill, C. K., Tong, A., Kawamura, D., Hayashi, A., Hunter, D. A., Parsadanian, A., Myckatyn, T. M. (2007). Reinnervation of the tibialis anterior following sciatic nerve crush injury: A confocal microscopic study in transgenic mice. *Experimental Neurology*, 207(1), 64–74. https://doi.org/10.1016/j.expneurol.2007.05.028
20. Siparsky, P. N., Kirkendall, D. T., & Garrett, W. E. (2014, January). Muscle Changes in Aging: Understanding Sarcopenia. *Sports Health*, Vol. 6, pp. 36–40. https://doi.org/10.1177/1941738113502296
21. Zhao, J., Tian, Z., Kadomatsu, T., Xie, P., Miyata, K., Sugizaki, T., … Oike, Y. (2018). Age-dependent increase in angiopoietin-like protein 2 accelerates Skeletal muscle loss in mice. *Journal of Biological Chemistry*, *293*(5), 1596–1609. https://doi.org/10.1074/jbc.M117.814996
22. Romanick, M., Thompson, L. D. V., & Brown-Borg, H. M. (2013, September 1). Murine models of atrophy, cachexia, and sarcopenia in skeletal muscle. *Biochimica et Biophysica Acta - Molecular Basis of Disease*, Vol. 1832, pp. 1410–1420. https://doi.org/10.1016/j.bbadis.2013.03.011
23. Painter, M. W. (2017, December 1). Aging Schwann cells: mechanisms, implications, future directions. Current Opinion in Neurobiology, Vol. 47, pp. 203–208. https://doi.org/10.1016/j.conb.2017.10.022
24. Venezie, R. D., Toews, A. D., & Morell, P. (1995). Macrophage recruitment in different models of nerve injury: Lysozyme as a marker for active phagocytosis. Journal of Neuroscience Research, 40(1), 99–107. https://doi.org/10.1002/jnr.490400111